ACCOUNTS of chemical research

Article

pubs.acs.org/accounts

Experimental and Theoretical Investigations of Energy Transfer and Hydrogen-Bond Breaking in Small Water and HCl Clusters

Amit K. Samanta,[†] Gábor Czakó,[§] Yimin Wang,[‡] John S. Mancini,[‡] Joel M. Bowman,*[,‡] and Hanna Reisler*[,†]

[†]Department of Chemistry, University of Southern California, Los Angeles, California 90089, United States

[‡]Department of Chemistry and Cherry L. Emerson Center for Scientific Computation, Emory University, Atlanta, Georgia 30322, United States

[§]Laboratory of Molecular Structure and Dynamics, Institute of Chemistry, Eötvös University, P.O. Box 32, H-1518 Budapest 112, Hungary

CONSPECTUS: Water is one of the most pervasive molecules on earth and other planetary bodies; it is the molecule that is searched for as the presumptive precursor to extraterrestrial life. It is also the paradigm substance illustrating ubiquitous hydrogen bonding (H-bonding) in the gas phase, liquids, crystals, and amorphous solids. Moreover, H-bonding with other molecules and between different molecules is of the utmost importance in chemistry and biology. It is no wonder, then, that for nearly a century theoreticians and experimentalists have tried to understand all aspects of H-bonding and its influence on reactivity. It is somewhat surprising, therefore, that several fundamental aspects of H-bonding that are particularly important for benchmarking theoretical models have remained unexplored experimentally. For example, even the binding strength between two gas-phase water molecules has never been determined with sufficient accuracy for comparison with high-level electronic structure calculations. Likewise, the effect of cooperativity (nonadditivity) in small H-bonded networks is not known with sufficient accuracy. An even greater challenge for both theory and experiment is the description of the dissociation dynamics of H-bonded small clusters upon acquiring vibrational excitation. This is because of the long lifetimes of many clusters, which requires running classical trajectories for many nanoseconds to achieve dissociation. In this Account, we describe recent progress and ongoing research that demonstrates how the combined and complementary efforts of theory and experiment are enlisted to determine bond dissociation energies (D_0) of small dimers and cyclic trimers of water and HCl with unprecedented accuracy, describe dissociation dynamics, and assess the effects of cooperativity. The experimental techniques rely on IR excitation of H-bonded X−H stretch vibrations, measuring velocity distributions of fragments in specific rovibrational states, and determining product state distributions at the pair-correlation level. The theoretical methods are based on high-level *ab initio* potential energy surfaces used in quantum and classical dynamical calculations.

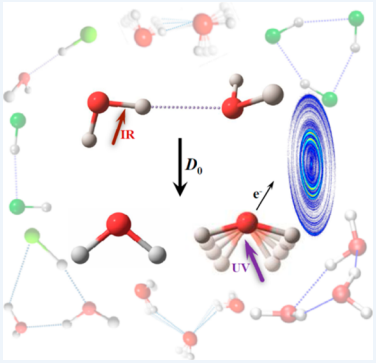

We achieve excellent agreement on D_0 between theory and experiments for all of the clusters that we have compared, as well as for cooperativity in ring trimers of water and HCl. We also show that both the long-range and the repulsive parts of the potential must be involved in bond breaking. We explain why H-bonds are so resilient and hard to break, and we propose that a common motif in the breaking of cyclic trimers is the opening of the ring following transfer of one quantum of stretch excitation to form open-chain structures that are weakly bound. However, it still takes many vibrational periods to release one monomer fragment from the open-chain structures. Our success with water and HCl dimers and trimers led us to embark on a more ambitious project: studies of mixed water and HCl small clusters. These clusters eventually lead to ionization of HCl and serve as prototypes of acid dissociation in water. Measurements and calculations of such ionizations are yet to be achieved, and we are now characterizing these systems by adding monomers one at a time. We describe our completed work on the HCl−H_2O dimer and mention our recent theoretical results on larger mixed clusters.

INTRODUCTION

Hydrogen is the most abundant element in the universe, and the hydrogen bond (H-bond) is the most pervasive and important noncovalent bond in nature. It is the bond responsible for the double-helical structure in DNA[1] and the structure of ice.[2] The study of H-bonding continues to be an active, perhaps more active than ever, area of research, experimentally and theoretically, even though it gained wide recognition after Pauling published his book on chemical bonding in 1939.[3] It is inherently difficult to define this important complex phenomenon simply, and a detailed summary of the existing knowledge and criteria has been proposed in a recent IUPAC document.[4]

Several basic aspects of the making and breaking of H-bonding networks remain unexplored, and this Account

Received: June 5, 2014
Published: July 29, 2014

dx.doi.org/10.1021/ar500213q | Acc. Chem. Res. 2014, 47, 2700−2709

describes how this research has benefited from our joint experimental and theoretical studies of binding strengths and bond-breaking mechanisms. Specifically, our work focuses on several benchmark H-bonded systems, namely, the water dimer and trimer, the HCl trimer, and the HCl−H_2O dimer. The structures of these H-bonded clusters and their binding energies (D_e) have been known to high accuracy for over a decade; however, their bond dissociation energies, D_0, which include zero-point energies (ZPE) of cluster and fragments, have only recently been measured and calculated with high accuracy and rigor. Note that D_e describes the minimum of the potential energy surface (PES) and cannot be measured experimentally. Recent studies have also allowed us to obtain a quantitative measure of another important yet subtle property of H-bonds, namely, cooperativity, i.e., nonadditivity. The accurate determination of D_0 of cyclic trimers provides a direct and quantitative measure of this nonadditivity. The breaking and rearrangement of H-bonds is another area of great interest, but there is very little work on dynamics published on these issues for small clusters.[5,6] For example, the unzipping of DNA, which is a prelude to replication, is another term for the breaking of H-bonds. In liquid water, the breaking of H-bonds is a prelude to hydration of ions and biomolecules.

Our joint work has focused specifically on the dissociation energy and dynamics of breaking H-bonds in the water and HCl clusters using state-of-the-art experimental and theoretical methods. We review the results of these studies here after a brief description of the essential aspects of the experimental and theoretical methods used in our joint research.

EXPERIMENTAL METHODS

The experimental methods allow accurate determination of D_0 of clusters and energy disposal in products. They are summarized in ref 6, which includes references to individual papers, and only a brief description is given here. Vibrational predissociation (VP) of specific clusters formed in a pulsed supersonic beam at 10−20 K rotational temperature is affected by IR excitation of H-bonded stretch vibrations with sufficient energy to produce monomer fragments. Fragments in selected rovibrational states are ionized via an excited electronic state that provides rotational resolution using (2 + 1) resonance enhanced multiphoton ionization (REMPI). Ions are detected mass-selectively with a position sensitive detector, which allows determination of velocity distributions of recoiling fragments using the velocity map imaging technique.[7]

For our experiments to be successful, several requirements must be met: (i) the desired cluster IR spectrum must be separated from the monomer and other clusters. Its detection efficiency depends on sample concentration, expansion conditions, IR laser fluence and focusing conditions, background signals, and so forth (see representative IR spectrum in Figure 1). (ii) A reliable REMPI detection scheme must exist for at least one of the monomer fragments and display isolated rovibrational levels suitable for imaging. For HCl, we use the excited $f\ ^3\Delta_2$ (v = 0) and $V\ ^1\Sigma^+$ (v = 11, 12) states as intermediates. The REMPI spectra of water are complicated by fast predissociation (short lifetimes) of the excited electronic states and spectral congestion,[8] and we developed detection schemes for H_2O and D_2O in their ground (000) and bending (010) states by excitation via the $\tilde{C}^1B_1$ state (Figure 2).[9] (iii) The velocity distributions obtained for each monitored fragment level should exhibit distinct structural features and/or clear energy cutoffs that can be used to determine D_0 accurately. Dynamical information about the VP is extracted from the velocity distributions and the rovibrational state distributions of the detected fragment(s), as described below. The experimental scheme is illustrated in Figure 3, which shows cluster excitation and fragment detection for $(H_2O)_3$.

The relative rovibrational state populations of the detected fragment are determined by scanning the REMPI excitation wavelength. The rovibrational distribution of the undetected fragment (pair-correlated cofragment) is extracted from the velocity distribution obtained for each image. This is accomplished by assigning a Gaussian-shaped curve (whose width is determined by the experimental velocity resolution) to

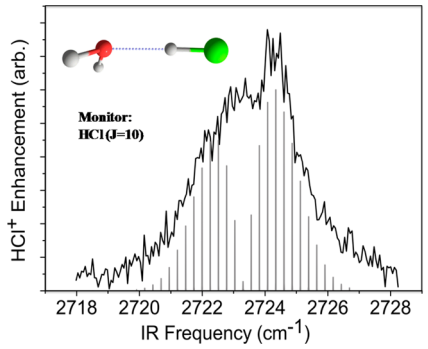

Figure 1. IR action spectrum of the HCl−H_2O dimer in the HCl stretch region, obtained by monitoring HCl (J = 10) fragment while scanning the IR laser frequency, with a simulated stick spectrum showing positions of rotational levels.

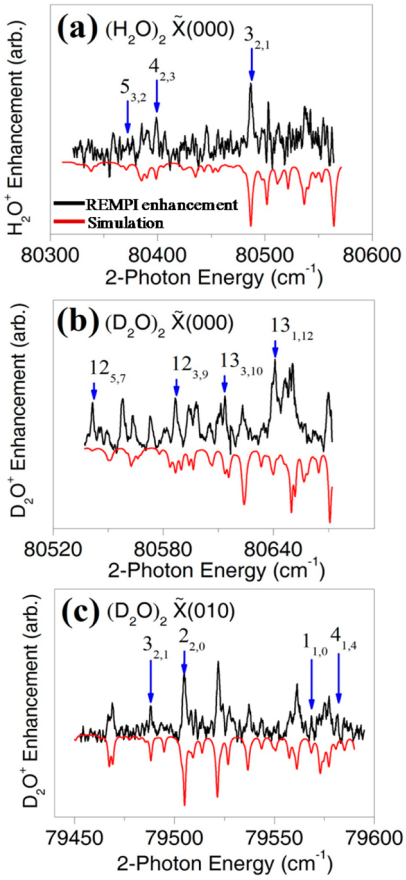

Figure 2. REMPI spectra and simulations of (a) $(H_2O)_2$ and (b, c) $(D_2O)_2$.

dx.doi.org/10.1021/ar500213q | Acc. Chem. Res. 2014, 47, 2700−2709

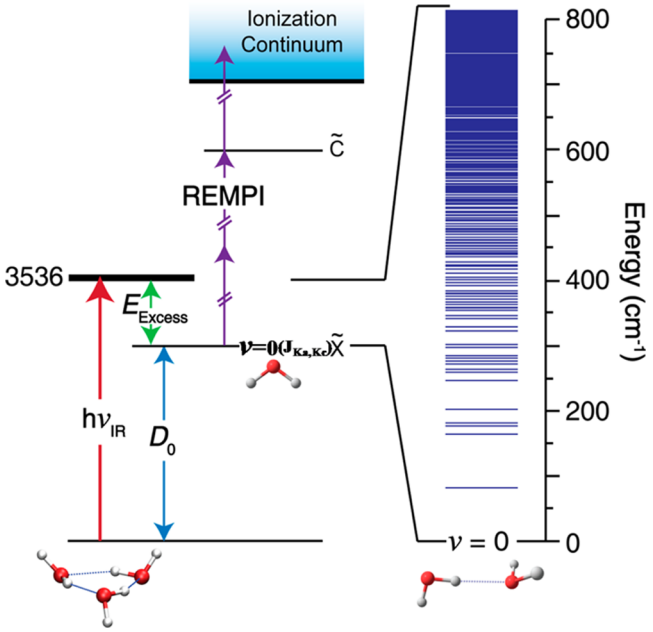

Figure 3. Experimental scheme for $(H_2O)_3$. The expanded energy level diagram represents vibrational states of the $(H_2O)_2$ cofragment.

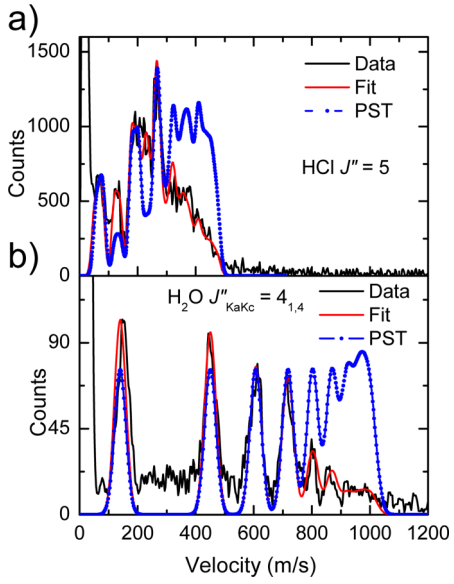

Figure 4. Velocity distributions obtained by monitoring (a) HCl and (b) H_2O from VP of HCl–H_2O at 2723 cm^{-1} and comparisons with PST. The peak near zero velocity is associated with monomer background in the monitored level.

each rotational level of each cofragment vibrational state. The positions of these Gaussians are determined by conservation of energy

$$h\nu_{IR} + E_{rot}(\text{cluster}) = D_0 + E_{vib,rot}(\text{mon}) + E_{vib,rot}(\text{cofrag}) + E_T$$

where E_{rot}(cluster) is the internal energy of the cluster estimated from fitting its IR spectrum, $h\nu_{IR}$ is the photon energy that induces VP, E_T is the measured center-of-mass (c.m.) translational energy obtained from the measured velocity distribution, and $E_{vib,rot}$(mon) and $E_{vib,rot}$(cofrag) are the rovibrational energies of the monitored fragment and the cofragment, respectively. $E_{vib,rot}$(mon) is known, and $E_{vib,rot}$(cofrag) is obtained from fitting the structures in the velocity distribution. The technique is best illustrated in the VP of HCl–H_2O, where water is probed state selectively, and each velocity distribution shows well-resolved features representing rotational levels of the HCl cofragment (Figure 4).[10]

As D_0 must remain constant for images obtained by monitoring different fragment rovibrational levels and the structures in the velocity distributions vary from image to image, the requirement of fitting an array of images with the same value of D_0 imposes severe restrictions on the acceptable D_0 values. In addition, by determining the total rovibrational state distributions as well as pair-correlated ones, stringent tests of dissociation models, such as the statistical phase space theory (PST), become possible.[11]

THEORETICAL METHODS

The theoretical/computational treatment of the dynamics of the clusters uses full-dimensional PESs that dissociate to molecular fragments. These are based on fitting high-level *ab initio* electronic energies, and they can be and have been used in calculations of bound vibrational dynamics as well as unbound dissociation dynamics. Here, the bound vibrational dynamics is limited to a rigorous determination of the ZPE and wave function of the cluster and dissociated products. This is needed to calculate D_0 accurately. For a study of the predissociation dynamics, a quasiclassical trajectory (QCT) treatment is employed, with quantization of the final states of the fragments. A brief description of the methods used to obtain the PESs is given next, followed by a brief description of the nuclear dynamics.

Potential Energy Surfaces

PESs have been developed using a convergent many-body representation, where the body is a monomer in a cluster. The general expression for the PES for N identical monomers at a general configuration of intra- and intermolecular coordinates is

$$V(1, 2, 3, ..., N) = \sum_{i=1}^{N} V_M(i) + \sum_{i<j=1}^{N} V_{2b}(i, j) + \sum_{i<j<k=1}^{N} V_{3b}(i, j, k) + ...$$

where the summations are for 1-body monomer potential, intrinsic 2-body, 3-body, and, in principle, higher-body interactions. This expression applies to pure water or HCl clusters. For mixed clusters, e.g., $(HCl)_n(H_2O)_m$, and using shorthand notation (H for HCl and W for H_2O), the expression for the PES is

$$V(H_n, W_m) = \sum_{i=1}^{n} V_H(i) + \sum_{i=1}^{m} V_W(i) + \sum_{i<j=1}^{n} V_{HH}(i, j) + \sum_{i<j=1}^{m} V_{WW}(i, j) + \sum_{i=1}^{n}\sum_{j=1}^{m} V_{WH}(i, j) + \sum_{i<j<k=1}^{n} V_{HHH}(i, j, k) + \sum_{i<j<k=1}^{m} V_{WWW}(i, j, k) + \sum_{i<j=1}^{n}\sum_{k=1}^{m} V_{HHW}(i, j, k) + \sum_{i=1}^{n}\sum_{j<k=1}^{m} V_{HWW}(i, j, k) + ...$$

where V_{HH} is the HCl 2-body interaction, V_{HW} is the HCl/H_2O 2-body interaction, and so forth. These expressions contain

dx.doi.org/10.1021/ar500213q | Acc. Chem. Res. 2014, 47, 2700–2709

explicit 1-, 2-, and 3-body interactions. For the dimers and trimers considered here, this truncation at the 3-body interactions is exact. Potentials up to 3-body interactions have been reported by the Bowman group for H_2O[12] and HCl[13] and also for H_2O–HCl.[14,15] The 1-body potentials are spectroscopically accurate monomer potentials; the 2- and 3-body water potentials are fits of roughly 40 000 CCSD(T)/aug-cc-pVTZ and 40 000 MP2/aug-cc-pVTZ energies. For HCl, the 2-body potential is obtained from the spectroscopically adjusted *ab initio* PES of Zhang and Bačić,[16] which was based on the earlier PES of Elrod and Saykally.[17] The potentials V_{WW}, V_{WWW}, V_{HHH}, V_{WWH}, and V_{WHH} are least-squares fits of roughly 40 000 electronic energies using permutationally invariant fitting bases.[18] This ensures that the mathematical representation of the PES is invariant with respect to all permutations of like atoms. However, with the necessary assignment of monomers, the potentials are effectively invariant with respect to all permutations of the monomers. It is noteworthy that the dimensionality of the 3-body potential is 12 for $(HCl)_3$ and 21 for $(H_2O)_3$ and so the mathematical fits are truly high-dimensional. The potentials for trimers dissociate accurately to dimer + monomer limits and also to three monomers; this is essential for dynamical studies.

Dynamics Calculations

Calculations of D_0 and dissociation dynamics of clusters were done using different approaches. The former requires an accurate D_e, calculated by taking the difference of the absolute energies of the complex and the dissociation products. Then, D_0 is computed by adding to D_e the difference between the complex and dissociated systems' ZPEs. The calculation of the ZPE of the monomer fragment is easily done with a variety of quantum methods. For dimers and trimers, the vibrational spaces are high-dimensional and so Diffusion Monte Carlo (DMC) calculations of ZPE were performed. These are computationally feasible using global potentials. These calculations follow the procedures described elsewhere,[19] and specific details for the water and HCl clusters are given in refs 12–15.

Dynamics of the predissociation of the clusters to fragments were described using QCT calculations. The detailed implementation depends somewhat on the cluster considered; however, the general approach is to use the normal-mode description of the cluster vibrational modes at global minimum, to give all modes ZPE, and for the mode excited experimentally additional vibrational energy equal to the photon excitation energy. In the present cases, this is the H-bonded O–H or Cl–H stretch. Roughly 10^4 trajectories, with microcanonical sampling of the initial phase space, were propagated for sufficiently long times to achieve dissociation. Then, the relative translational energy and internal energies of the fragments were determined. Details for $(H_2O)_2$,[9] $(H_2O)_3$,[20] and $(HCl)_3$[21] have been published.

GEOMETRIES AND PROPERTIES OF CLUSTER GROUND STATES

The global minimum structures of $(H_2O)_2$ and $(H_2O)_3$ as well as $(HCl)_3$ and H_2O–HCl have been accurately established by us and others (see refs 12–15 for relevant earlier literature). More insight is obtained from a depiction of the rigorous zero-point wave functions, as shown in Figure 5. As expected, the dimers, with a single H-bond, are floppier than the trimers, where three H-bonds confine the trimer to tight ring. It is interesting to note that the maximum in the zero-point wave function for HCl–H_2O is not at the global minimum but at a planar structure, which has energy roughly 50 cm^{-1} above the global minimum.[14] Thus, properties of this cluster, such as the zero-point rotational constants and the HCl fundamental excitation, are not accurately obtained using the global minimum structure. Instead, they are obtained accurately using the planar structure, as discussed elsewhere.[15]

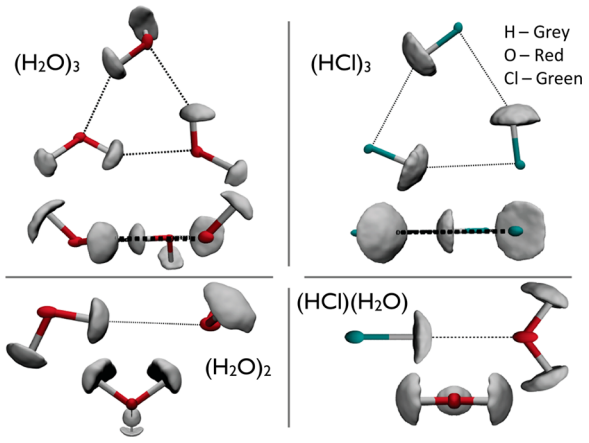

Figure 5. Isosurface representations of the indicated clusters.

DISSOCIATION ENERGIES

An accurate calculation of D_0 requires an accurate D_e and ZPEs. The former was obtained using complete basis-set (CBS) extrapolation of so-called gold standard coupled cluster energies with large basis sets, as described before.[12−14] The accurate ZPEs were obtained by the methods described above using the fitted PESs. Note that the D_e of these PESs is generally within tens of reciprocal centimeters of the CBS result.

The Experimental Methods described above give D_0 values with ±10 cm^{-1} accuracy for clusters for which distinct structures appear in the velocity distributions. For example, by using D_0 = 1334 cm^{-1}, the velocity distributions in Figure 4 could be fit very well with rotational levels of (a) water and (b) HCl cofragments. Likewise, Figure 6 depicts typical fragment velocity distributions obtained by monitoring specific vibrational and $J_{Ka,Kc}$ fragment levels for $(H_2O)_2$ and $(D_2O)_2$ from which D_0 values were determined accurately.[9] The values are listed in Table 1, and the agreement with theory in all cases is excellent.

Extending the measurements to trimers is challenging because of the increasing density of states of the cofragments, which often results in velocity distributions with no structures. In trimers made of diatomic molecules, however, the density of states is lower. Figure 7 shows several velocity distributions obtained following 2810 cm^{-1} Cl–H vibrational excitation of $(HCl)_3$.[21] Depending on the monitored HCl(J), energy is available either to form only the monomer + dimer (channel I; J = 11) or, for J < 11, both channels I and II (three HCl fragments). The J = 11 velocity distribution is structured, because there are relatively few internal states of $(HCl)_2$ that are correlated with it. This enables determination of D_0 for channel I, which is then used to fit images that include contributions from channels I and II and to determine D_0 for channel II accurately. As shown in Table 1, agreement with theory is excellent.

dx.doi.org/10.1021/ar500213q | Acc. Chem. Res. 2014, 47, 2700−2709

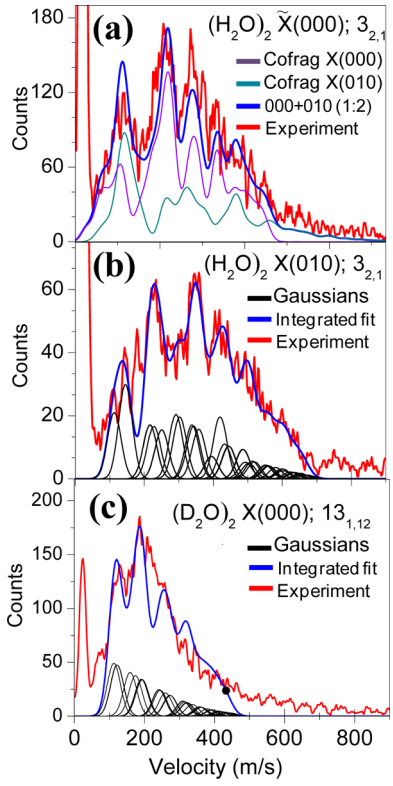

Figure 6. Velocity distributions obtained by monitoring state-selected (a, b) H_2O and (c) D_2O fragments.

Table 1. D_0 Values in Wavenumbers from Theory and Experiment

system	theory	experiment
$(H_2O)_2 \rightarrow 2(H_2O)$	1104 ± 5	1105 ± 10
$(D_2O)_2 \rightarrow 2(D_2O)$	1244 ± 5	1244 ± 10
$(H_2O)_3 \rightarrow (H_2O)_2 + (H_2O)$	2726 ± 30	2650 ± 150
$(H_2O)_3 \rightarrow 3(H_2O)$	3855 ± 20	
$(HCl)_2 \rightarrow 2(HCl)$	431 ± 1	439 ± 1
$(HCl)_3 \rightarrow HCl + (HCl)_2$	1133 ± 2	1142 ± 20
$(HCl)_3 \rightarrow 3(HCl)$	1564 ± 1	1545 ± 10
$(HCl)(H_2O) \rightarrow HCl + H_2O$	1348 ± 3	1334 ± 10

A less satisfactory situation, but probably more typical for larger clusters, is illustrated by $(H_2O)_3$, for which the state-selective velocity distributions show no structures (Figure 8).[20] Nevertheless, by assuming a statistical energy distribution in the $(H_2O)_2$ cofragment (there is not enough energy to produce three monomers) and fitting multiple images, reasonable agreement with theory is achieved (Table 1). The justification for using statistical distributions is given below and elsewhere.[20]

Accurate D_0 also helps to assess the contributions of cooperativity to the binding in H-bonded networks, as described below.

■ COOPERATIVITY

The importance of cooperativity in H-bonded networks was already recognized in understanding the properties of water. Nevertheless, there were very few experiments that assessed this contribution accurately. Our studies provide the first comparison of experiment and theory for the smallest networks: the ring trimers of HCl and water. For ejection of one monomer from a ring trimer, cooperativity is given simply

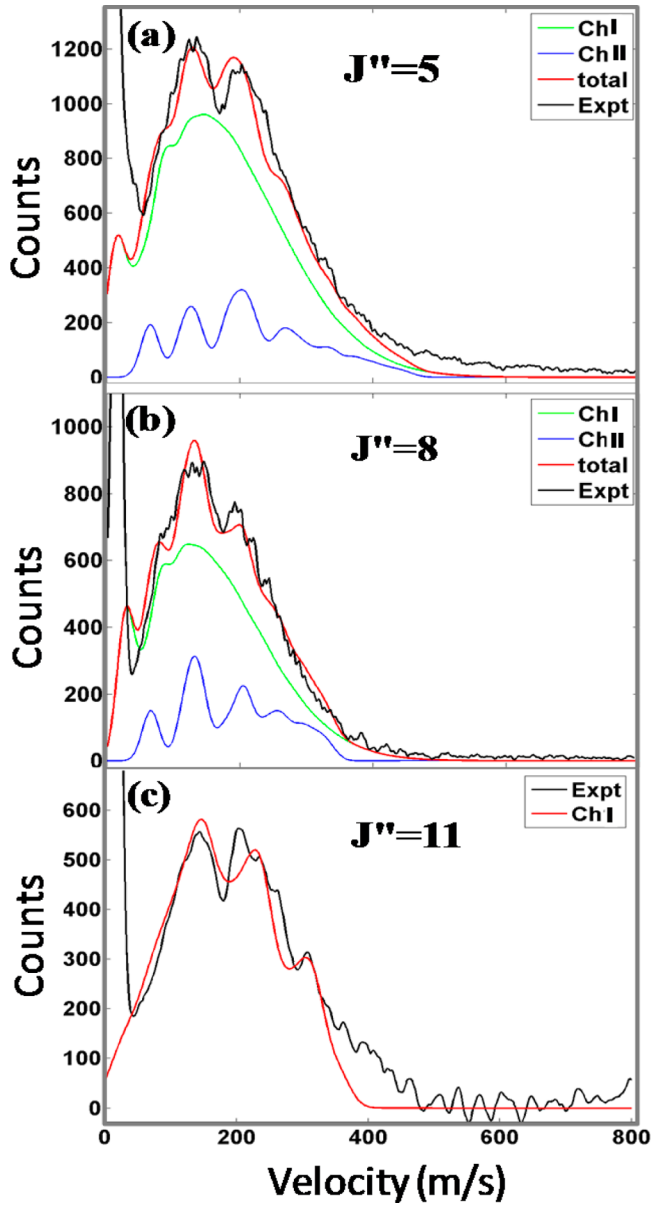

Figure 7. Velocity distributions of HCl fragments from $(HCl)_3$.

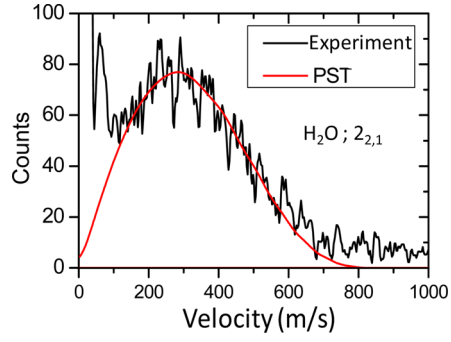

Figure 8. Velocity distribution of H_2O fragments from $(H_2O)_3$.

by D_0(trimer) − $2D_0$(dimer). The experimental value for $(HCl)_3$ is ~250 cm^{-1}, in good agreement with the theoretical values of ~251 and ~271 cm^{-1} obtained by two theoretical methods.[21] The corresponding value for $(H_2O)_3$ is ~450 cm^{-1}.[20] These are 22 and 19% of the total binding energy of the

dx.doi.org/10.1021/ar500213q | Acc. Chem. Res. 2014, 47, 2700−2709

monomer to the dimer for HCl and H_2O, respectively. These large contributions are surprising in view of the considerable ring strain and the significant deviations from the optimal dimer geometry (linear for water and T-shaped for HCl). Nevertheless, it is clear that the greatest contribution to cooperativity comes from the binding of the monomer to the dimer.

In principle, we rely on theory to shed light on the origins of the cooperative contributions. Because these appear to be true many-body effects, beyond long-range polarization, this is a challenge for theory and an active area of research, see, e.g., ref 22.

CLUSTER LIFETIMES

It has been established by spectroscopic studies that dissociation lifetimes of van der Waals and H-bonded clusters can be as long as nanoseconds. The long lifetimes reflect the weak coupling of the excited high-frequency intramolecular modes to low-frequency modes, and they present a challenge for dynamics calculations because trajectories have to be followed up for a long time, and many trajectories do not achieve dissociation.

The bottleneck to energy transfer is the initial coupling of the excited X−H stretch vibration to other inter- and intramolecular modes. An illustrative example is $(HCl)_3$, which lives for more than 10 ns before dissociation.[23] Spectroscopy and theory indicate that it is difficult to couple the Cl−H stretch vibration to intermolecular cluster modes.[21,23] Once the stretch energy is transferred to ring modes, it takes picoseconds for the ring to open, finally releasing a monomer. Theory shows that when depositing the energy in one HCl unit of the ring, it takes picoseconds for the stretch energy to start delocalizing over the three monomers. The resonant energy transfer among the three HCl stretches and a simple Hückel theory analysis of it is given elsewhere.[13,23] The delocalized vibrational excitation then slowly relaxes to intermolecular modes. The nanosecond relaxation to those modes is difficult to describe with a simple model; however, ring opening most often precedes dissociation. This is seen in both $(HCl)_3$ and $(H_2O)_3$; however, relaxation is significantly faster (tens of picoseconds) in $(H_2O)_3$[24] than in $(HCl)_3$. This is likely due to the additional intramolecular bend mode in H_2O that acts as a doorway to relaxation to the intermolecular modes. This has recently been demonstrated in quantum calculations of rapid (sub picosecond) vibrational relaxation of HOD in ice.[25]

VIBRATIONAL PREDISSOCIATION DYNAMICS

Energy Disposal in Dimers

The propensity rules of Ewing for VP rates provide guidelines to energy disposal.[26] They rely on momentum (or energy) gap laws and predict a preference for fragment channels for which the number of transferred quanta to the dissociation mode is small. This leads to a preference for fragment vibrational excitation over rotational excitation over translational energy (E_T) release. Because a small change in the number of vibrational quanta leads to a large decrease in available energy, vibrational energy transfer is favored, although the state specificity observed in vibrational excitation remains unexplained.[6] Rotational excitation is more favorable than E_T release in VP of dimers whose fragments have large rotational constants.

The weak couplings between intra- and intermolecular vibrations give rise to nonstatistical VP dynamics and state specificity in fragments' rovibrational populations. However, exit-channel couplings can modify initial distributions, especially when energy differences between rotational levels are small. This can lead to statistical-like rotational distributions, which usually still deviate from statistical predictions by exhibiting enhanced populations of high *J*s. These propensities are clearly revealed in the pair-correlated rotational distributions obtained in the VP of HCl−H_2O. In Figure 4, the velocity distributions of HCl and H_2O cofragments are compared to predictions of PST. PST applies only conservation of energy and angular momentum and assumes that all allowed states are equally populated. The under-population of low rotational fragment levels corresponding to high velocities is evident. Similar propensities are seen in the monomer fragments' rotational distributions in $(H_2O)_2$ and $(D_2O)_2$ VP.[9]

Another issue is how the excess energy is shared between donor−acceptor. In heterodimers, this can be addressed experimentally, and state specificity in vibrational energy disposal is often seen.[6] For homodimers, the question can be answered only by theory, as demonstrated for $(H(D)_2O)_2$.[9] Here, the experimental and theoretical results are complementary. Imaging experiments provide pair-correlated product state distributions, whereas the QCT calculations give the distributions in each fragment. Following H-bonded O−H(D) stretch excitation, both fragments can be formed in the ground (000) state, or one fragment can have one quantum of bending (010) excitation. What the experiments cannot establish, but is revealed in calculations, is that the rotational distributions in the original donor and acceptor fragments in both dissociation channels of $(H_2O)_2$ and $(D_2O)_2$ are similar.

In addition, the QCT calculations predict, in agreement with experiment, that the predominant VP channel in $(H_2O)_2$ and $(D_2O)_2$ is (000) + (010).[9] Theory shows that following excitation of H-bonded O−H(D) stretch of the donor, vibrational energy is first shared between donor and acceptor vibrational levels, leading to equal probability of bending excitation in the donor and acceptor and similar rotational state distributions. Snapshots of a representative $(H_2O)_2$ trajectory are shown in Figure 9, which shows that exchanges of donor and acceptor indeed occur several times before dissociation.

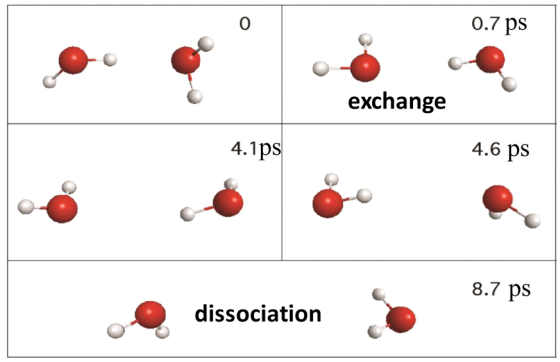

Figure 9. $(H_2O)_2$ trajectory leading to dissociation.

Although the initial pathways of energy transfer out of the excited O−H(D) stretch are not yet fully elucidated, the first step likely involves coupling to two quanta of intramolecular bend and one or more intermolecular vibrations, as there are near-resonant pathways for such couplings.[9] This energy must then transfer to the intermolecular modes, including the dissociation coordinate. This step is inefficient and most often

dx.doi.org/10.1021/ar500213q | Acc. Chem. Res. 2014, 47, 2700−2709

leaves a quantum of bending excitation in one fragment. For $(D_2O)_2$, contributions from high rotational levels in the (000) fragments are observed that have similar energies to the (010) bending level.[9] This minor channel may result from processes in which the excited dimer samples the repulsive part of the PES in an impulsive interaction, converting both bending quanta into fragment rotation and translation and accessing high rotational levels.

Energy Disposal in the Ring Trimers of Water and HCl

The smallest fully H-bonded networks are the ring trimers, which can break into two possible fragmentation channels: monomer + dimer and three monomers. Referring to the monomer + dimer channel of $(H_2O)_3$, we expect product energy distributions to be more statistical than in dimers due to the larger vibrational density of states of the dimer fragment (Figure 3). Therefore, we compared the observed velocity distributions in the VP of $(H_2O)_3$ to predictions of the statistical PST calculations as well as to QCT calculations. Figure 10a shows good agreement between the measured E_T distribution and the distribution obtained by QCT calculations. Moreover, the QCT distribution agrees well with the distribution obtained by PST (Figure 10b). This is easily rationalized by the large intermolecular vibrational density of states of the $(H_2O)_2$ fragment.

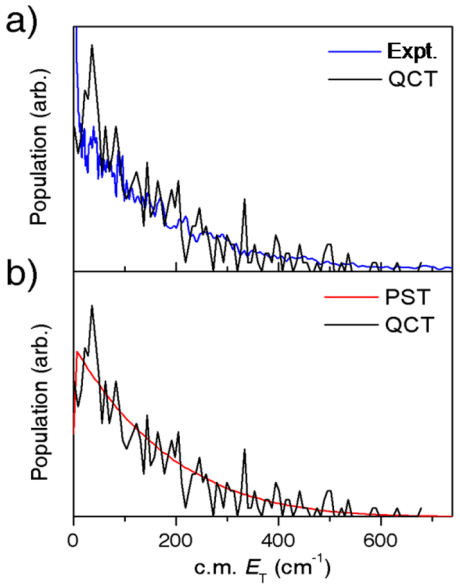

Figure 10. Comparison of E_T distribution obtained from QCT (J = 2–4) with (a) experimental distribution of H_2O ($J_{Ka,Kc}$ = $3_{2,1}$) fragments and (b) statistical distribution obtained by PST.

The trajectories show, as expected, many vibrational oscillations in the trimer prior to dissociation. The ring opens early on in the trajectory and then reforms and breaks numerous times (often with different H-bonds breaking) until finally the second H-bond breaks and H_2O fragments appear. Ring opening always precedes dissociation.

To gain further insight into the dissociation mechanism of cyclic trimers, we studied $(HCl)_3$ because it allowed us to examine both primary fragmentation channels: HCl + $(HCl)_2$ (channel I) and 3HCl (channel II). The reason for this is that D_0 of $(HCl)_2$ is small (439 cm^{-1})[27] and $(HCl)_3$ excitation at 2810 cm^{-1} provides sufficient energy for total fragmentation. In previous spectroscopic studies of HF, DF, and HCl trimers,[23,28] it was proposed that the first step in the dissociation is the opening of the ring.

Because of the smaller density of fragment states in $(HCl)_3$, we were able to gain more information about the HCl(J) distributions and the pair-correlated velocity distributions for each channel. The HCl(J) distributions were obtained by REMPI and agree well with calculations (Figure 11). Both are broad and encompass all of the allowed rotational levels.

Figure 12 displays the E_T distributions, derived from velocity distributions of HCl fragments in different J levels, along with the corresponding distributions obtained by QCT calculations for Channel I (the major channel). While the experimental and theoretical distributions match quite well for J = 10, they deviate progressively more as J decreases, with the greatest mismatch for J = 5. This is a reasonable result because some dimer fragments have internal energies that exceed their dissociation energy of 439 cm^{-1}.[27] These dimers further dissociate into two monomers that have E_T distributions extending from the maximum allowed energetically down to very low E_Ts. We denote the dissociation of these "hot" fragments as Channel Ia: $[(HCl)_2]^{**} \rightarrow$ HCl + HCl. As expected, the contribution of Channel Ia decreases in going from J = 5 to 8, as the latter has a smaller fraction of dimer cofragments with the requisite high internal energies. Indeed, the best agreement between theory and experiment is obtained for J = 10.[21]

The theoretical calculations show that the rate-limiting step in the VP is the relaxation of the Cl–H stretch excitation to the intermolecular modes of the trimer. Once the stretch relaxes, one H-bond can break, and the ring can transition to a stable open-chain configuration, 737 cm^{-1} higher in energy. The minimum energy path for this conformational change is demonstrated in Figure 13. The time spent in the open-chain conformer allows energy to further localize in the H-bonds. After the trimer explores the open-chain conformer for a significant length of time, the excitation energy fully localizes in two of the H-bonds, breaking them and forming a monomer and dimer (Channel I).[21]

Both theory and experiment indicate that $(HCl)_2$ fragments from Channel I have broad distributions of rovibrational energies, which resemble a microcanonical distribution. This channel leads first to monomer + dimer, and then some of the hot dimers further dissociate to monomers. Finally, the experiments show a small contribution from direct decomposition to three monomers, which does not proceed via the open-chain structure. This Channel II is responsible for the distinct structures seen in some of the velocity distributions, and data analysis indicates that it does not proceed via sequential breaking of H-bonds as observed in Channels I and Ia but rather via a single-step mechanism that involves the concerted breakup of all three H-bonds.[21] The latter channel, however, which has been seen only in the experiments, does not contribute significantly, and the sequential mechanism remains the dominant process.

■ CONCLUSIONS AND FUTURE DIRECTIONS

The excellent agreement between theory and experiment for bond dissociation energies and energy distributions is gratifying. Although H-bonding in water has been known for about a century, the bond dissociation energy between two isolated water molecules, the most fundamental unit, has not been measured precisely before. Likewise, it is only recently that theoretical treatment of floppy clusters with flexible monomers

dx.doi.org/10.1021/ar500213q | Acc. Chem. Res. 2014, 47, 2700–2709

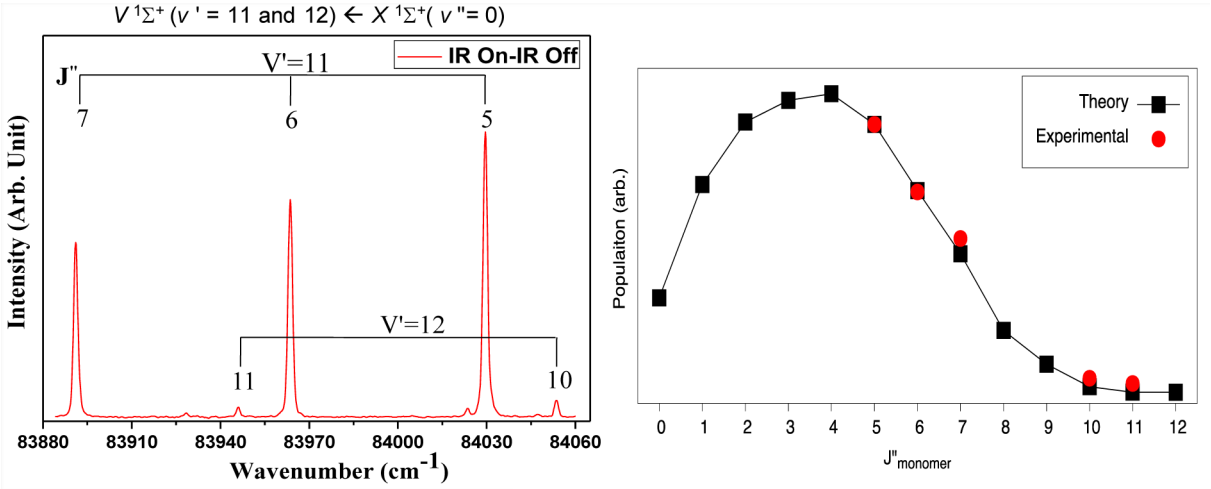

Figure 11. HCl fragment 2 + 1 REMPI spectrum (left) and comparison (right) of theoretical and experimental HCl rotational populations.

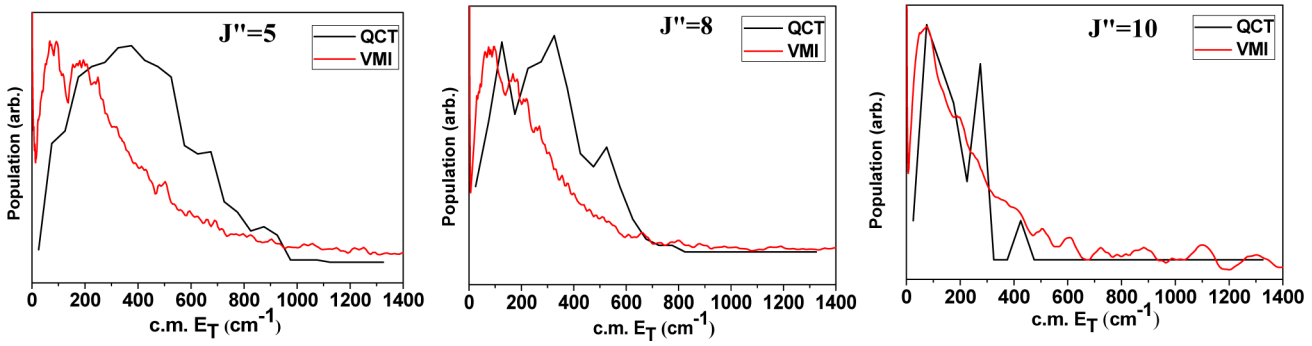

Figure 12. E_T distributions obtained by detecting HCl fragments (red) and corresponding distributions obtained from QCT calculations for Channel I (black) for J = 5 (left), 8 (middle), and 10 (right).

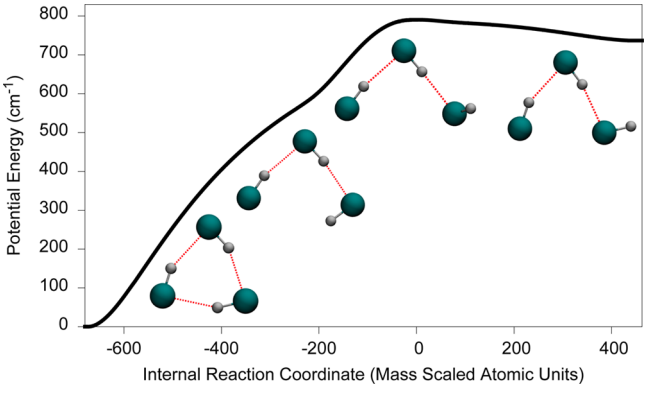

Figure 13. Minimum energy path from cyclic $(HCl)_3$ (left) to open-chain configuration (right).

has reached the level required to calculate D_0 accurately. The value presented in Table 1 for $(H_2O)_2$, which has now been incorporated into the interactive thermochemical tables,[29] can be used to improve other thermochemical values, such as the proton affinity of water to give H_3O^+.[30] Because measuring D_0 for larger clusters becomes ever more challenging, it is important to use benchmark cases to demonstrate the reliability of calculations and to understand how to extend them to larger systems. Calculations of D_0 are relatively straightforward with the availability of full-dimensional PESs because DMC calculations can be done for fairly large clusters. For the larger H-bonded networks, it is as important to assess the contributions of cooperative interactions to the binding. Our studies of the ring trimers of water and HCl show that cooperativity contributions are quite large, about ∼20% for dissociation energy to monomer + dimer, even in cases where ring strain and deviations from ideal dimer geometries are large. On the basis of analysis of many-body contributions to the binding energies of water clusters done by us and very thoroughly by others,[22] it does appear that 3-body contributions to the cooperativity continue to dominate even for large clusters.

In VP of dimers, fragment internal state distributions are usually nonstatistical.[5,6] Rotational state distributions range from an extreme in which a single pair of fragment J states dominates to minimize E_T release, as in $(HCl)_2$,[27] to $(H_2O)_2$, in which, due to the smaller separation between rotational levels, the final fragment distributions are broad and encompass all of the energetically allowed J states. Fragment vibrational populations exhibit state specificity that probably depends on the details of the PES, existence of accidental resonances, and so forth. As expected, product state distributions from VP of trimers are more statistical and populate all of the allowed rotational levels. This reflects either more extensive IVR and/or strong exit-channel interactions.

Common to the dimers and trimers is their long lifetimes, ranging from tens of picoseconds to nanoseconds. This presents a challenge for dynamics calculations. It appears, however, that the most important dynamical features are captured by starting the calculations from the open-chain

dx.doi.org/10.1021/ar500213q | Acc. Chem. Res. 2014, 47, 2700−2709

structure. As proposed before, the rate-limiting step is the coupling of the excited X−H stretch to other intra- and intermolecular cluster modes. The open-chain intermediates may therefore appear as a common motif in the breakup of cyclic clusters. Also, as shown for $(HCl)_3$, even when sufficient energy is available for breakup to three monomers, the sequential route is more important than concerted dissociation.

We have begun studies of $(HCl)_m(H_2O)_n$ clusters,[14,15] which have been the focus of intense experimental and theoretical research recently. A full-dimensional PES has been developed for the HCl−H_2O dimer, and the calculated D_0 is in good agreement with experiment (Table 1).[6] We have recently developed *ab initio* full-dimensional intrinsic 3-body potentials for $(HCl)_2H_2O$ and $HCl(H_2O)_2$, which, together with previous 1-, 2-, and 3-body potentials, permit a description of general $(HCl)_m(H_2O)_n$ clusters prior to the formation of H_3O^+ and Cl^-.[15] (We note that the generation of 3-body potentials to study the ionized clusters is in progress.) The recently developed potentials have been used in vibrational configuration interaction calculations of the HCl and OH-stretch fundamentals, and agreement with experiment is very good for the clusters $(HCl)(H_2O)$, $(HCl)(H_2O)_2$, $(HCl)(H_2O)_3$, $(HCl)_2H_2O$, $(HCl)_2(H_2O)_2$, and $(HCl)_3(H_2O)$.[14,15] Predissociation dynamics studies of these clusters can now be done both theoretically using these potentials and experimentally using the techniques described here. Preliminary results of IR action spectra for $(HCl)(H_2O)_2$ obtained by detecting HCl and H_2O fragments show good agreement with theory.

AUTHOR INFORMATION

Corresponding Authors

*(J.M.B.) E-mail: joel.bowman@emory.edu.
*(H.R.) E-mail: reisler@usc.edu.

Notes

The authors declare no competing financial interest.

Biographies

Amit K. Samanta obtained his B.Sc. and M.Sc. degrees in Chemistry from the University of Calcutta, India, and his Ph.D. from the Indian Association for the Cultivation of Science (IACS), India. He is now a postdoctoral researcher at USC.

Gábor Czakó received his Ph.D. in theoretical chemistry at Eötvös University, Budapest, Hungary, in 2007. He was a postdoctoral fellow at Emory University, and he is currently a research associate at the Institute of Chemistry, Eötvös University.

Yimin Wang received her B.S. degree in Chemistry from USTC, China, and her Ph.D. degree from Emory University. She is currently a postdoctoral fellow at Emory University.

John S. Mancini received his B.S. degree in Chemistry from Richmond University. He is now a graduate student at Emory University.

Joel M. Bowman received his A.B. degree from the University of California, Berkeley, and his Ph.D. from the California Institute of Technology. His is currently a Professor of Chemistry at Emory University.

Hanna Reisler received her B.Sc. and M.Sc. degrees from Hebrew University and her Ph.D. from the Weizmann Institute of Science in Israel. She was a postdoctoral fellow at Johns Hopkins University and is now a Professor of Chemistry at USC.

ACKNOWLEDGMENTS

We thank Andrew K. Mollner, Blithe E. Rocher, and Lee C. Ch'ng for their essential contributions and discussions. This work was supported by U.S. National Science Foundation grant nos. CHE-1265725 (H.R.) and CHE-1145227 (J.M.B.) and the Scientific Research Fund of Hungary (OTKA, NK83583) (G.C.).

REFERENCES

(1) Watson, J. D.; Crick, F. H. C. Structure for Deoxyribose Nucleic Acid. *Nature* **1953**, *171*, 737−738.
(2) Ludwig, R. Water: From Clusters to the Bulk. *Angew. Chem., Int. Ed.* **2001**, *40*, 1808−1827.
(3) Pauling, L. *The Nature of the Chemical Bond and the Structure of Molecules and Crystals: An Introduction to Modern Structural Chemistry*; Cornell University Press: New York, 1939.
(4) Arunan, E.; Desiraju, G. R.; Klein, R. A.; Sadlej, J.; Scheiner, S.; Alkorta, I.; Clary, D. C.; Crabtree, R. H.; Dannenberg, J. J.; Hobza, P.; Kjaergaard, H. G.; Legon, A. C.; Mennucci, B.; Nesbitt, D. J. Defining the Hydrogen Bond: An Account (IUPAC Technical Report). *Pure Appl. Chem.* **2011**, *83*, 1619−1636.
(5) Oudejans, L.; Miller, R. E. Photofragment Translational Spectroscopy of Weakly Bound Complexes: Probing the Interfragment Correlated Final State Distributions. *Annu. Rev. Phys. Chem.* **2001**, *52*, 607−637.
(6) Samanta, A. K.; Ch'ng, L. C.; Reisler, H. Imaging Bond Breaking and Vibrational Energy Transfer in Small Water Containing Clusters. *Chem. Phys. Lett.* **2013**, *575*, 1−11.
(7) Eppink, A.; Parker, D. H. Velocity Map Imaging of Ions and Electrons Using Electrostatic Lenses: Application in Photoelectron and Photofragment Ion Imaging of Molecular Oxygen. *Rev. Sci. Instrum.* **1997**, *68*, 3477−3484.
(8) Yang, C. H.; Sarma, G.; ter Meulen, J. J.; Parker, D. H.; Western, C. M. REMPI Spectroscopy and Predissociation of the $\tilde{C}^1B_1$ (v = 0) Rotational levels of H_2O, HOD and D_2O. *Phys. Chem. Chem. Phys.* **2010**, *12*, 13983−13991.
(9) Ch'ng, L. C.; Samanta, A. K.; Czakó, G.; Bowman, J. M.; Reisler, H. Experimental and Theoretical Investigations of Energy Transfer and Hydrogen-Bond Breaking in the Water Dimer. *J. Am. Chem. Soc.* **2012**, *134*, 15430−15435.
(10) Rocher-Casterline, B. E.; Mollner, A. K.; Ch'ng, L. C.; Reisler, H. Imaging H_2O Photofragments in the Predissociation of the HCl−H_2O Hydrogen-Bonded Dimer. *J. Phys. Chem. A* **2011**, *115*, 6903−6909.
(11) Pechukas, P.; Light, J. C. On Detailed Balancing and Statistical Theories of Chemical Kinetics. *J. Chem. Phys.* **1965**, *42*, 3281−3291.
(12) Czakó, G.; Wang, Y.; Bowman, J. M. Quasiclassical Trajectory Calculations of Correlated Product-State Distributions for the Dissociation of $(H_2O)_2$ and $(D_2O)_2$. *J. Chem. Phys.* **2011**, *135*, 151102.
(13) Mancini, J. S.; Bowman, J. M. A New Many-Body Potential Energy Surface for HCl Clusters and Its Application to Anharmonic Spectroscopy and Vibration−Vibration Energy Transfer in the HCl Trimer. *J. Phys. Chem. A* **2014**, DOI: 10.1021/jp412264t.
(14) Mancini, J. S.; Bowman, J. M. A New Ab Initio Potential Energy Surface for HCl−H_2O, Diffusion Monte Carlo Calculations of D_0 and a Delocalized Zero-Point Wavefunction. *J. Chem. Phys.* **2013**, *138*, 121102.
(15) Mancini, J. S.; Bowman, J. M. Effects of Zero-Point Delocalization on the Vibrational Frequencies of Mixed HCl and Water Clusters. *J. Phys. Chem. Lett.* **2014**, *5*, 2247−2253.
(16) Qiu, Y.; Zhang, J. Z. H.; Bačić, Z. Six-Dimensional Quantum Calculations of Vibration-Rotation-Tunneling Levels of ν_1 and ν_2 HCl-Stretching Excited $(HCl)_2$. *J. Chem. Phys.* **1998**, *108*, 4804−4816.
(17) Elrod, M. J.; Saykally, R. J. Vibration−Rotation−Tunneling Dynamics Calculations for the Four-Dimensional $(HCl)_2$ System: A Test of Approximate Models. *J. Chem. Phys.* **1995**, *103*, 921−932.

(18) Braams, B. J.; Bowman, J. M. Permutationally Invariant Potential Energy Surfaces in High Dimensionality. *Int. Rev. Phys. Chem.* **2009**, *28*, 577−606.
(19) McCoy, A. B. Diffusion Monte Carlo Approaches for Investigating the Structure and Vibrational Spectra of Fluxional Systems. *Int. Rev. Phys. Chem.* **2006**, *25*, 77−107.
(20) Ch'ng, L. C.; Samanta, A. K.; Wang, Y.; Bowman, J. M.; Reisler, H. Experimental and Theoretical Investigations of the Dissociation Energy (D_0) and Dynamics of the Water Trimer, $(H_2O)_3$. *J. Phys. Chem. A* **2013**, *117*, 7207−16.
(21) Mancini, J. S.; Samanta, A. K.; Bowman, J. M.; Reisler, H. Experiment and Theory Elucidate the Multichannel Predissociation Dynamics of the HCl Trimer: Breaking up Is Hard to Do. *J. Phys. Chem. A* **2014**, DOI: 10.1021/jp5015753.
(22) Cobar, E. A.; Horn, P. R.; Bergman, R. G.; Head-Gordon, M. Examination of the Hydrogen-Bonding Networks in Small Water Clusters (n = 2−5, 13, 17) Using Absolutely Localized Molecular Orbital Energy Decomposition Analysis. *Phys. Chem. Chem. Phys.* **2012**, *14*, 15328−15339.
(23) Fárník, M.; Nesbitt, D. J. Intramolecular Energy Transfer Between Oriented Chromophores: High-Resolution Infrared Spectroscopy of HCl Trimer. *J. Chem. Phys.* **2004**, *121*, 12386.
(24) Keutsch, F. N.; Cruzan, J. D.; Saykally, R. J. The Water Trimer. *Chem. Rev.* **2003**, *103*, 2533−2578.
(25) Liu, H.; Wang, Y.; Bowman, J. M. Ab Initio Deconstruction of the Vibrational Relaxation Pathways of Dilute HOD in Ice Ih. *J. Am. Chem. Soc.* **2014**, *136*, 5888−5891.
(26) Ewing, G. E. Selection Rules for Vibrational Energy Transfer: Vibrational Predissociation of van der Waals Molecules. *J. Phys. Chem.* **1987**, *91*, 4662−4671.
(27) Ni, H.; Serafin, J. M.; Valentini, J. J. Dynamics of the Vibrational Predissociation of HCl Dimer. *J. Chem. Phys.* **2000**, *113*, 3055.
(28) Michael, D. W.; Lisy, J. M. Vibrational Predissociation Spectroscopy of $(HF)_3$. *J. Chem. Phys.* **1986**, *85*, 2528−2537.
(29) Ruscic, B. Active Thermochemical Tables: Water and Water Dimer. *J. Phys. Chem. A* **2013**, *117*, 11940−11953.
(30) Bodi, A.; Csontos, J.; Kallay, M.; Borkar, S.; Sztáray, B. On the Protonation of Water. *Chem. Sci.* **2014**, *5*, 3057−3063.